



Growth of nacre in abalone: Seasonal and feeding effects

M.I. Lopez^{*}, P.Y. Chen, J. McKittrick, M.A. Meyers

University of California, San Diego, La Jolla, California, USA

ARTICLE INFO

Article history:

Received 20 March 2010

Received in revised form 16 July 2010

Accepted 3 September 2010

Available online 9 September 2010

Keywords:

Abalone
Nacre
Growth
Haliotis
Chitin
Biom mineralization

ABSTRACT

The processes of aggregation of mineral and organic materials to the growing surfaces in red abalone (*Haliotis rufescens*) are analyzed. The flat pearl implantation method is used to observe the transient stages of calcium carbonate deposition, the structure of the organic interlayer, and the steady-state growth of aragonite tiles. The morphology of the organic interlayer is characterized by scanning electron microscopy. These results enable a realistic depiction of the formation of the terraced cones that comprise the principal biomineralization mechanism in this gastropod. In all cases, the growth initiated through spherulites, followed by tile formation. The transient stage with spherulitic formation was shorter at higher temperature; this is indicative of a greater activity of the animal at 21 °C. The growth rate in a normally fed gastropod was found to be higher compared with one provided with limited food. The effect of water temperature (seasonal) was also established, with growth proceeding faster in the summer (T ~ 21 °C) than in winter (15 °C). The structures of the organic interlayer and of the epithelium are revealed by scanning electron microscopy.

Published by Elsevier B.V.

1. Introduction

Understanding the process in which living organisms control the growth of structured inorganic materials can inspire new and better synthetic materials [1–5]. Indeed, there have been recent successes in synthesizing a ceramic/polymer composite with outstanding toughness inspired by the structure of nacre in the abalone shell [6–9].

The growth of nacre is a well studied subject characterized by many researchers [10–35]. In particular, the growth and structure relationship has been studied in detail [16,20–24,31]. Results show that aragonite crystals first radiate from nucleation sites forming a spherulitic pattern, and then, columnar aragonite crystals form preferentially in the *c* direction (perpendicular to the growth surface). This morphology is then replaced by the aragonite tile pattern. Lin et al. [31] examined the structure during a period of 1 to 6 weeks. In the third week, the columnar growth still dominated and by the sixth week growth cones of the aragonite nacre became present. Furthermore, the role of the organic layer in the growth of the abalone nacre has been studied by Belcher et al. [22,23,26], Zaremba et al. [27], Sarikaya et al. [28–30], Lin et al. [15,31], Meyers et al. [16,17], and Bezares et al. [34,35], which has led to proposed mechanisms of growth.

However, little attention has been paid to factors that affect the development of these transient phases. Changes in the feeding patterns may limit the source of ions for mineral formation in the abalone shell. Moreover, changes in its environment, such as

temperature of the sea water, might affect the nucleation rate and growth rate of the transitory phases of calcium carbonate. Thus, the environment may play an important role in the mineral formation. Additionally, past studies suggest a large involvement of the mantle and epithelial cell layer to form the intricate structure of the growing front of the shell. Calcium radioisotope movement studies on the oyster *Crassostrea virginica* show that movement of the ⁴⁵Ca out of the mantle correlated with the amount of ⁴⁵Ca deposited on the shell growth front. Additional mollusk ion transport studies on the isolated mantle indicate ion movements from the mantle to the shell, while other studies suggest that Ca²⁺ transport occurs by diffusion through this mantle [38]. However, this process is not fully understood and studies of this soft tissue can give insights into this biomineralization process.

This study intends to investigate the process of mineralization following periods of growth interruption, taking into consideration important environmental factors (access to food and temperature) and to employ high-magnification characterization techniques to better understand how the soft tissue (e.g. epithelium and organic membrane) influences the mechanism of growth.

2. Experimental techniques

Two labeled red abalone (*Haliotis rufescens*) were held in a 45 liter fish tank in an open water facility at the Scripps Institution of Oceanography. The tank had direct access to continuously circulating sea water, providing a natural environment with steady pH. Animals were fed giant kelp (*Macrocystis pyrifera*) at different schedules and the mean temperature was controlled. Three experiments were carried out, varying average temperature and feeding rate of the

^{*} Corresponding author.

E-mail address: mil032@ucsd.edu (M.I. Lopez).

animal (Table 1). The ‘flat pearl’ technique, first used in the US by the U.C. Santa Barbara group [20,21,25,27] and latter applied by Lin et al. [31], was utilized to extract specimens for growth observations. Circular glass slides (15 mm in diameter) were implanted in live abalone for periods of 1–3 weeks and then extracted weekly for examination. The mantle was pressed back (retracted) with a flat scalpel and the slides were glued to the growing edge of the animal (Fig. 1). The largest quantity of slides allowed by the size and surface of the animal was implanted on each abalone. In Fig. 1, six slides were implanted and are shown by arrows. Once securely adhered, the mantle relocated itself over slides over the period of approximately 24 h. At least one slide from each of the abalone was removed weekly and prepared for scanning electron microscopy (SEM) and atomic force microscopy (AFM) characterization.

For SEM preparation, the slides were air dried and sputter coated with gold-platinum. The specimens were observed both from top and cross-sectional perspectives in the environmental and in the high vacuum modes of the Phillips XL30 ESEM. The surface morphology of abalone nacre was also examined by AFM (Veeco Scanning Probe Microscope) in ambient dry condition.

The intercellular layer of mantle was also characterized. A small slice (~1 cm) cut was made on two sections of live abalone (Fig. 2). Then each section was re-sectioned into two parts. Samples were CO₂ critical point dried and gold-platinum coated for observation in the ESEM in high vacuum mode.

Sections from the growing edge of abalone shell were also cut, washed in deionized water and demineralized in 0.6 N HCl at 20 °C for 1 week. Specimens were then dehydrated completely in a progressive manner in ethanol and CO₂ critical point dried so that the structure was maintained. Sections were gold-platinum coated and observed in the ESEM high vacuum mode.

3. Results and discussion

3.1. Characterization of growth surfaces

The investigation in warm water (21 °C) revealed that the aragonite tiles formed after only 1 week (Fig. 3a). Furthermore, the folding organic layers which are approximately 300 nm thick (marked by arrows) can be observed. Conversely, in cold water (15 °C) (Fig. 3b) or with food limitation (20 °C) (Fig. 3c), observations after 1 week showed only the slight start of the precursor aragonite spread across the substrate and some of the deposited mineral transitioning to spherulitic aragonite. Slides from the second abalone were also observed and confirmed the same results. Moreover, week 2 demonstrated similar aragonite tiles (Fig. 4a) when the growth was conducted in warm water (21 °C). In contrast, uniform spherulitic aragonite was observed in cold water (15 °C) (Fig. 4b) or under no feeding conditions (20 °C) (Fig. 4c). Interestingly, the spherulitic aragonite observed when the animal was not fed tends to be less radiated compared to the structure in colder water. After 3 weeks of growth in warm water (21 °C), a uniform and high number of stacked aragonite tiles (terraced cones) were observed (Figs. 5a and b). It can be noted from Fig. 5a that because the height of the terraced cones is the same, an even terrain is formed. In addition, from this cross-sectional view, a continuous membrane formed by the organic layer can be observed. From Fig. 5b it can be noted that the top of the terraced cones appears to be of a consistent diameter (~400 nm). On



Fig. 1. Glass slides (depicted by arrows) embedded in abalone shell.

the contrary, after 3 weeks of implantation, the tops of each spherulitic bundle form a plateau for test at 15 °C (Fig. 5c) and test without feeding (20 °C) (Fig. 5d). In addition, the thin organic membrane can be observed (Fig. 5c).

AFM confirmed all the features observed by SEM. Fig. 6 shows the growth surface in 21 °C. These mineral projections (terraced cones) are approximately 2 μm high, depicting about four layers from the top of the cones. This corresponds to the thickness of the tiles, (~0.5 μm). One can also see in Fig. 6b, on the sides of the protrusion, which represent terraced cones, the organic interlayer in a tent-like formation. This is similar to the configurations seen in Figs. 3, 4 and 5, in which a thin organic layer covers terraced cones and demonstrates that the organic layer, in its fully hydrated condition, stretches under its own weight. On the other hand, it acquires substantial strength when it is dry [17]. In contrast to this, Fig. 7 demonstrates that only the spherulite morphology is attained with growth in water at 15 °C. Some distortion exists as the AFM tip does not capture very well the lateral details.

It should be clarified that the rate of the transition from initial randomly arranged CaCO₃, a spherulitic transient phase, to final aragonite tile growth reported here is not the growth rate of the nacre, which is also affected by temperature and food availability



Fig. 2. Abalone mantle pushed back revealing epithelium (depicted by arrow) prior to excision.

Table 1
Experimental conditions for sequential growth.

Condition	Temperature of water	Feeding schedule
1	~21 °C	Regularity
2	~15 °C	Regularity
3	~20 °C	Not fed

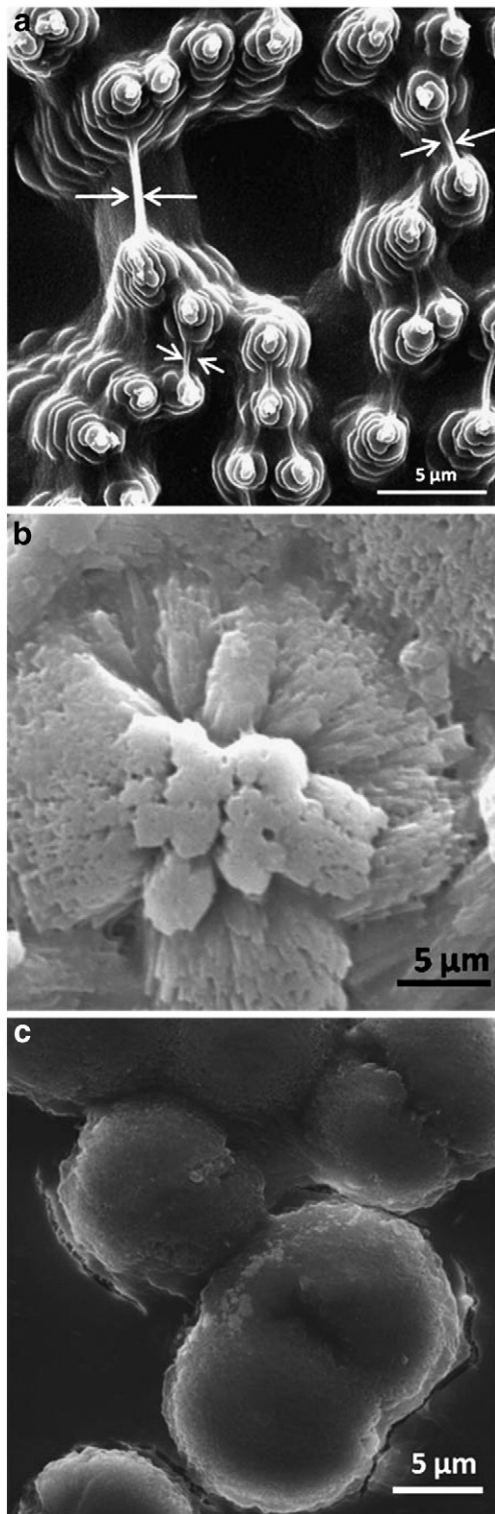


Fig. 3. Sequential growth results 1 week after implantation. a) Growth at 21 °C with abalone regularly fed; b) growth at 15 °C with abalone regularly fed; c) growth at 20 °C without food available.

[36]. Sequential growth results discussed by Lin et al. [31] demonstrated that the shell growth required various transitory phases to reach the steady-state growth of aragonite tiles. Aragonite tiles formation was achieved after approximately 6 weeks of precursor transitory phases (this previous study was performed at 15 °C and the animal was fed regularly). The growth surfaces (Figs. 3b and 4b) show dominating spherulitic pattern and columnar growth which is

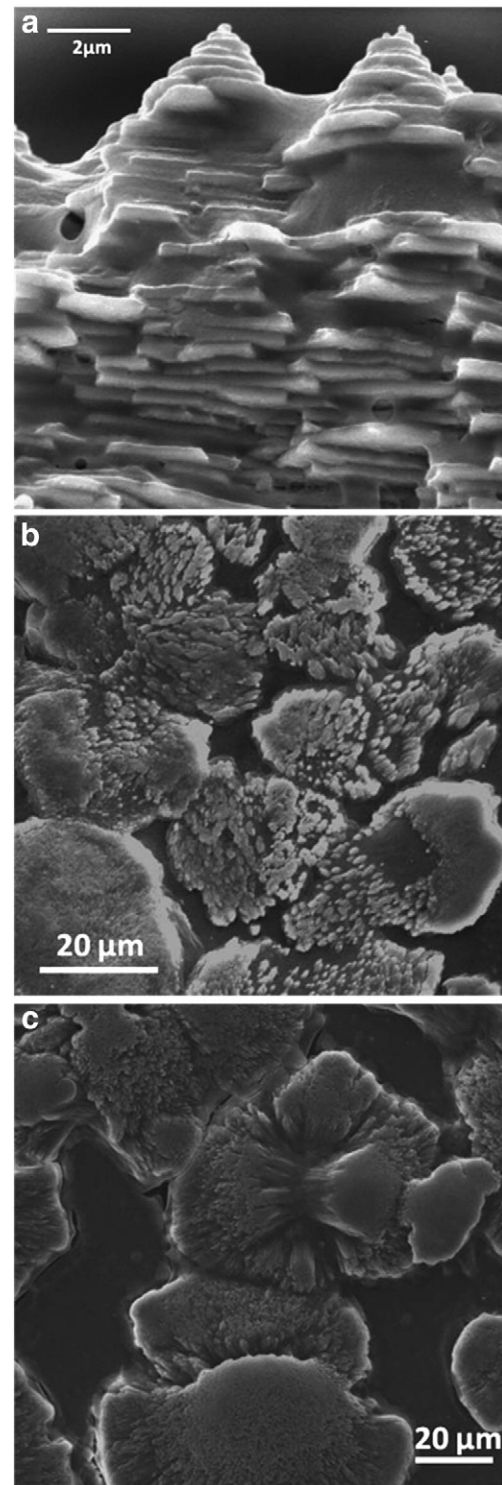


Fig. 4. Sequential growth results 2 weeks after implantation. a) Cross-sectional view of growth at 21 °C with abalone regularly fed; b) growth at 15 °C with abalone regularly fed; c) growth at 20 °C without feeding.

comparable to the results for 3 to 4 weeks described by Lin et al. [31].

In contrast, when the temperature was warmer (21 °C), the transitions occurred faster. At this temperature, the transitory phases cannot be observed as the steady-state growth of aragonite tiles is reached by week one. Additionally, when the animal was not fed, the transitions occurred later. The columns observed in the limited food

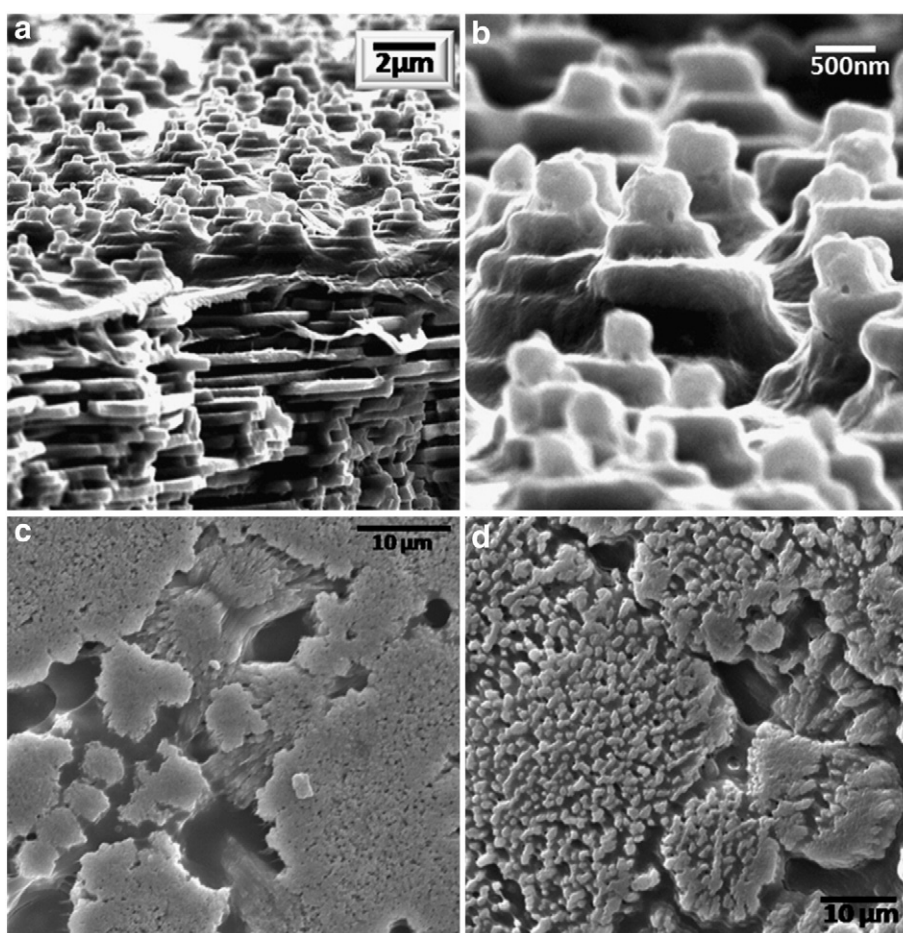


Fig. 5. Sequential growth results after 3 weeks of implantation. a) Growth at 21 °C with abalone regularly fed (cross-section); b) detailed view of aragonite tile morphology; c) growth in 15 °C with abalone regularly fed; d) growth in 20 °C without food available.

conditions at 20 °C tend to be less radiated and the surface less smooth when compared with the growth surfaces attained at 15 °C. It is believed that the predominant columnar growth of the aragonite mineral is interrupted by the deposition of thin organic intertile layer [17]. The lack of nutrients and lower temperature may reduce the production of the organic layer (chitin and proteins), which leads to an unimpeded rapid columnar growth instead of the steady-state growth of the aragonite tiles.

3.2. Epithelium observations

Inspection of the mantle reveals the secretory epithelium which is in direct contact with the inner surface of the shell (Fig. 8). This part of the animal is the critical component in the mineralization of the shell, since it is only separated from the growing surfaces by the small extrapallial space. SEM inspection (Fig. 8a) shows a top section of the outer surface of the epithelium (labeled I) and an area where the top surface is scraped off (labeled II). The relatively smooth outer surface of the epithelium (Fig. 8b) suggests that the epithelium mechanically flattens the growing surface by sliding over the shell, producing a molding effect [31] analogous to a potter molding clay. From the scraped surface one can observe that an array of channels exists inside the epithelium (detailed view of the channels shown in Fig. 8c). Some of these channels show fibrils (Fig. 8d). Lin et al. [31] and Meyers et al. [17] proposed that ions are allowed to diffuse through these channels. In addition, these channels may provide support for the synthesis of chitin and its intermittent extrusion onto the growth front (Fig. 9).

3.3. Demineralized shell and organic layer

The sectioned and demineralized shell samples from the growing edge revealed areas of thin organic intertile layer (Fig. 10a) in arrays of stretched holes. This organic intertile layer is believed to be periodically deposited (every ~0.5 μm) by the epithelium in the animal. It is composed of a thin biopolymer protein framework secreted by epithelial cells [37–41]. This organic layer is an important characteristic and has been studied successively [15–17,34,35]. Lin and Meyers [15] investigated the thicker regions (20 μm) of organic layer that exist between the shell's mesolayers. These thick layers are believed to be formed by seasonal fluctuations where calcification is interrupted. Subsequently, Meyers et al. [16] further noted the role of the organic matrix (20–50 nm thick) interlayer in the formation of the CaCO₃ aragonite matrix into 0.5 μm thick tiles. Moreover, Meyers et al. [17] showed further evidence of the chitin network that forms the structural component of the intertile layer and characterized it by SEM, AFM, and nanoindentation. Furthermore, Bezares et al. [34,35] described the structure of demineralized tissue and examined its mechanical response. In addition to being a key element in the excellent mechanical properties, it is also an important component in regulating the growth of the aragonite. This layer slows down the growth of the aragonite in the rapid growth (c axis) direction.

These results are in agreement with the growth mechanism proposed by Meyers and co-workers [17,31]. The growth of the mineral is allowed to proceed through the orifices in the organic layer as the transport of calcium and carbonate ions is permitted through the

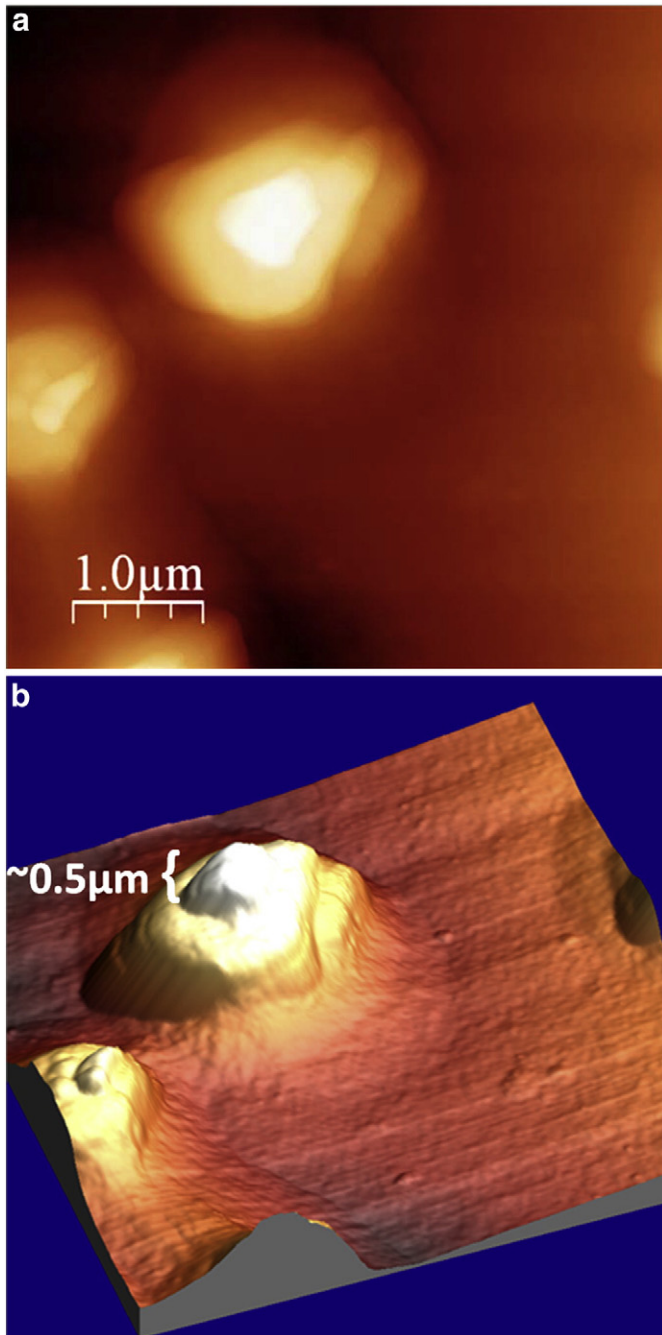


Fig. 6. Atomic force microscopy of growth surface in 21 °C showing the aragonite tile growth. a) Top view; b) tridimensional view.

holes in the organic layer (Fig. 10b). Fig. 11 shows randomly oriented chitin macromolecule fibrils [1,17,33,42–44] considered to be the structural component of the organic layer.

There are two hypotheses explaining the formation and growth of the tiles:

- Organic scaffold, into which Ca^{2+} and CO_3^{2-} ions penetrate, combine, and precipitate [e.g. 34,35].
- Periodic deposition of organic layer with holes, retarding the growth of aragonite crystals in the c direction (perpendicular to the growth surface) [17,31].

The organic scaffold hypothesis requires intricate genetic engineering. On the other hand, the periodic chitin deposition hypothesis is directly regulated by the mantle. The results obtained by Lin et al.

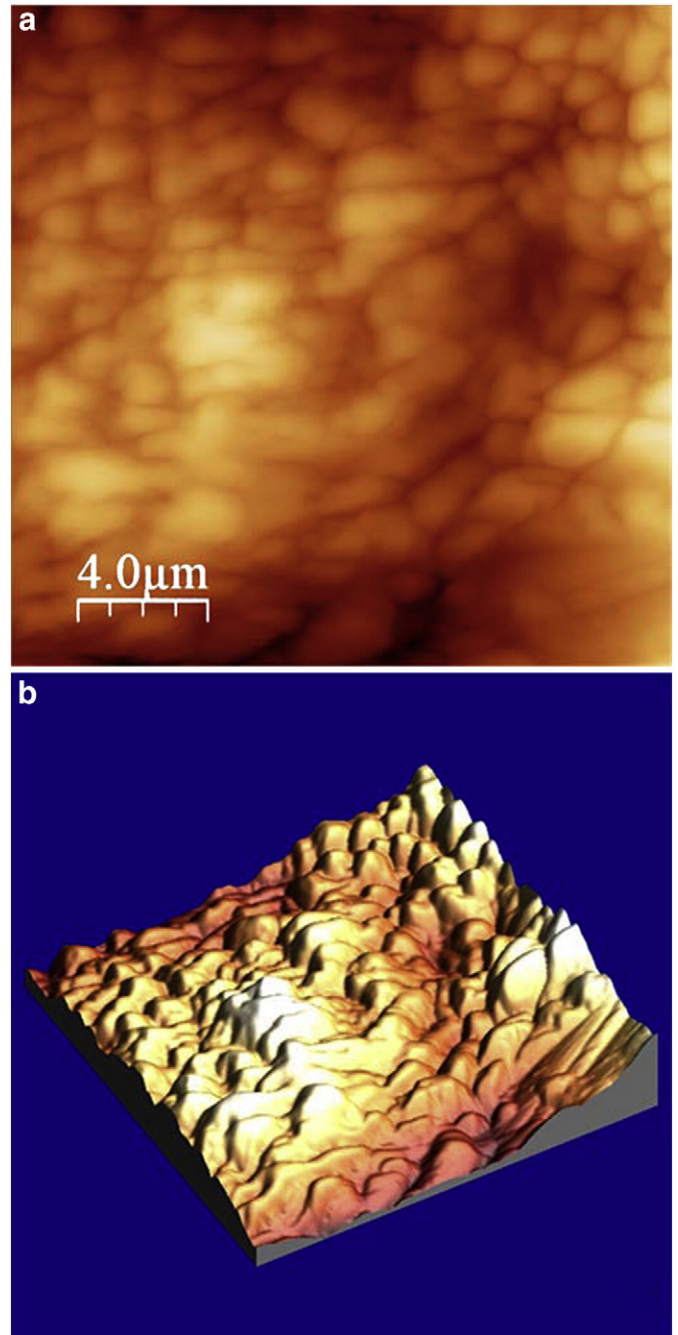


Fig. 7. Atomic force microscopy of growth surface in 15 °C showing the columnar structure. a) Top view; b) tridimensional view.

[31], Meyers et al. [17], and here strongly support the periodic deposition hypothesis, a mechanism well described by Schäffer et al. [25] and Belcher et al. [22,26]. Especially significant is the fact that the layers between laterally adjacent tiles are much thinner than the horizontal ones (parallel to the growth surface), as shown in Fig. 10b. Of importance also is the identification of chitin synthesis sites in the cavernous channels within the epithelium; it is proposed that they are extruded onto the growth surface by mechanical action from the abalone foot.

4. Conclusions

In this study, the growth process of abalone nacre under different environmental conditions (water temperature and food availability)

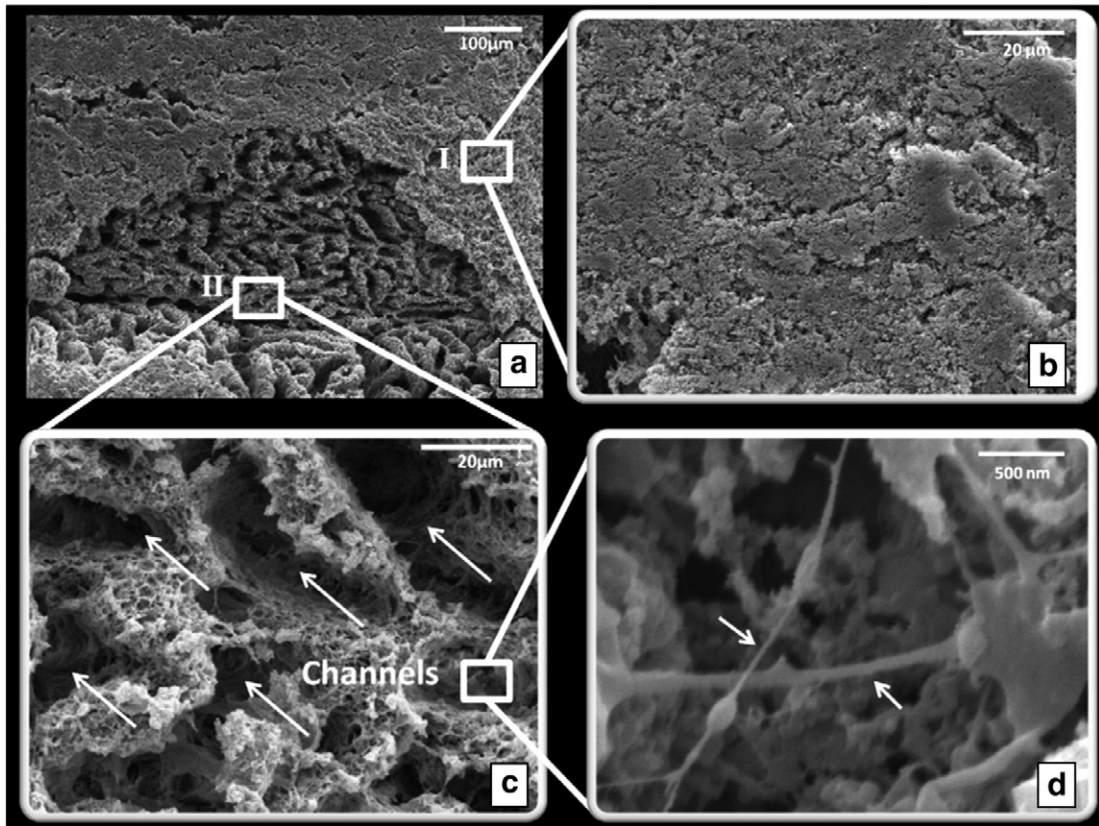


Fig. 8. a) Sectioned epithelium; surface in contact with growing edge of shell depicting flat outer surface (I) and area where surface scraped off (II); b) detailed view of flat outer surface of epithelium. c) Array of channels within epithelium (channels depicted by arrows); d) fibrils within channels (marked with arrows).

is investigated by the flat pearl technique combined with SEM and AFM observations. Demineralization studies were also performed. The major findings are:

1. The rate of the transition from an initial random nucleation to the steady-state growth of aragonite tiles in abalone nacre is greatly affected by water temperature and food availability. The aragonite tile growth is achieved faster at warmer water temperature (21 °C) compared with colder temperature (15 °C). The transition from columnar to aragonite tile growth takes longer when the food

supply is limited. It is proposed that the lack of nutrients and lower temperature may reduce the production of the intertile organic layer, which leads to columnar growth of mineral instead of the aragonite tiles.

2. An outer smooth surface and inner channels are observed in the epithelium. These channels provide a path for ion and chitin transport. The smooth outer surface is believed to mechanically flatten the growing surface of the shell.
3. The demineralized shell showed sections of the intertile layer and chitin network. This organic component is believed to influence

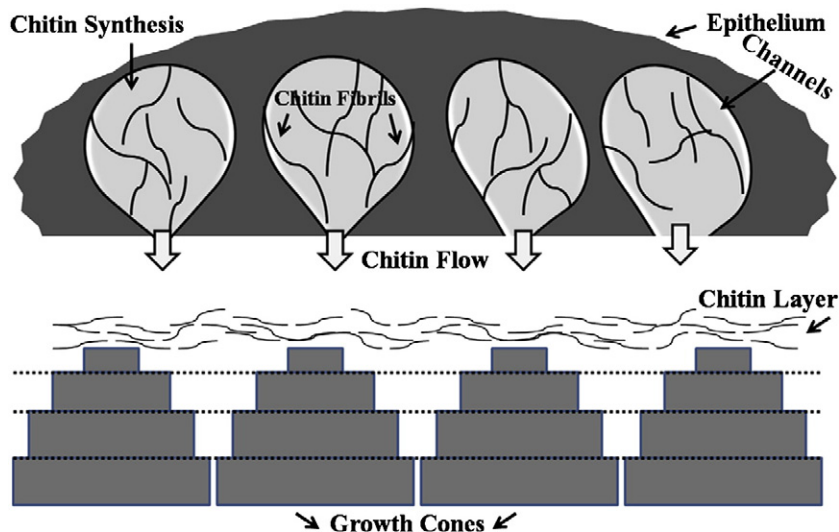


Fig. 9. Schematic depiction of hypothetical mechanism by which epithelium generates chitin fibrils and ‘squeezes’ them onto growth surface.

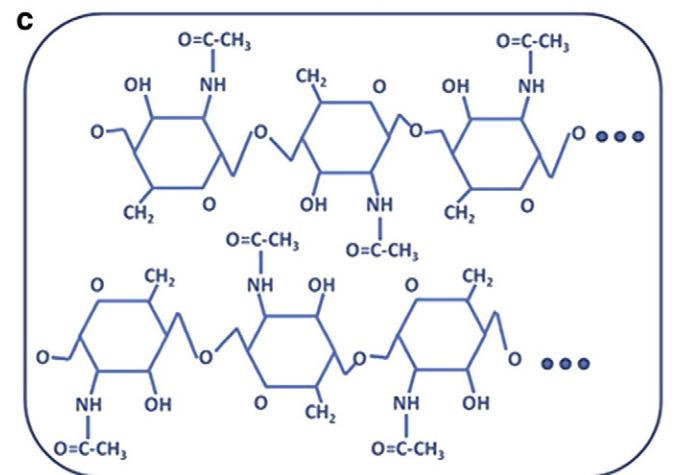
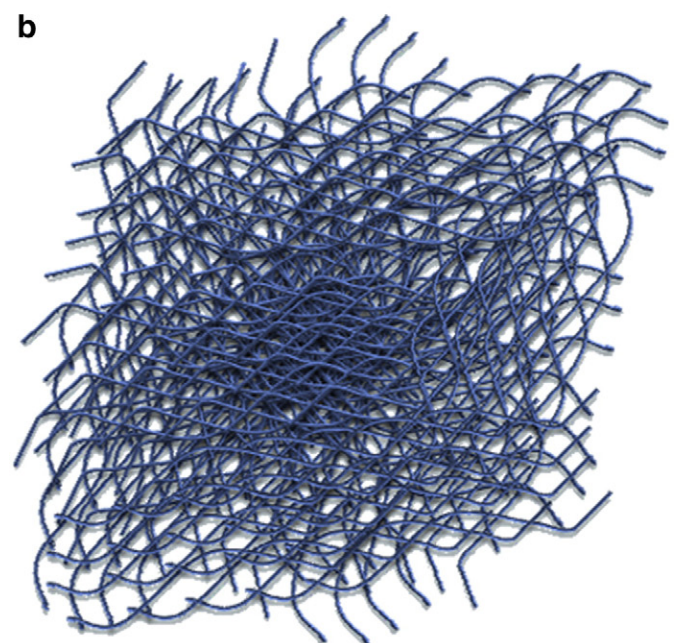
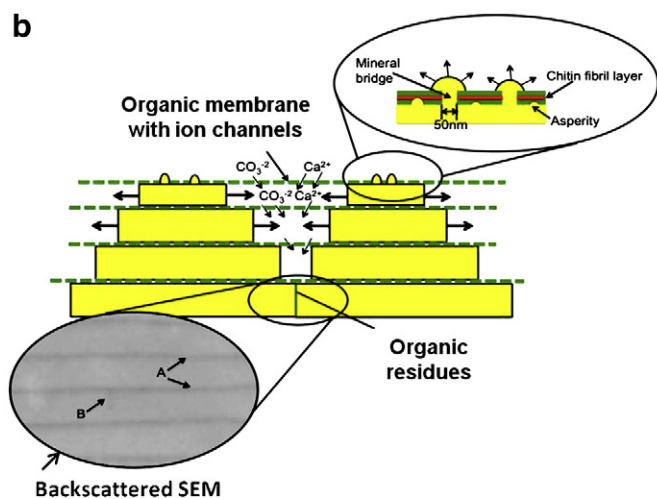
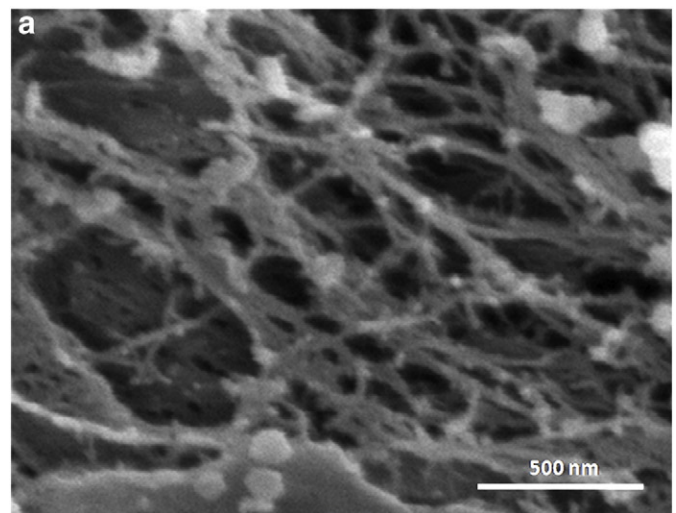
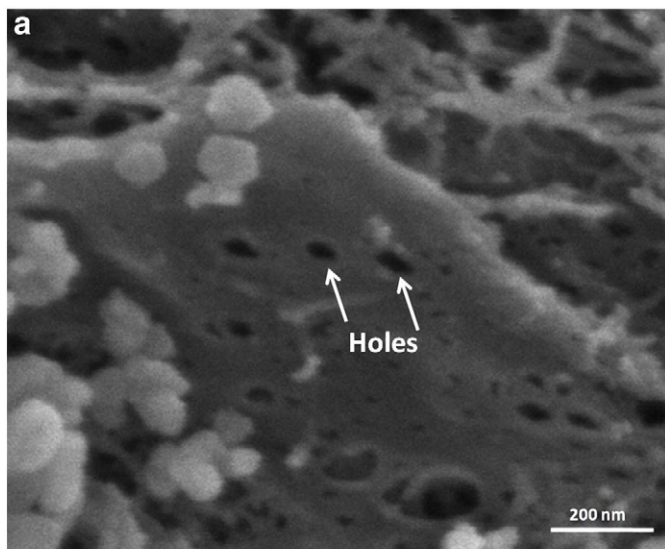


Fig. 10. a) Thin intertile organic layer showing holes; b) proposed mechanism of growth of nacreous tiles by formation of mineral bridges as depicted by Meyers et al. [17]; organic layer is permeable to calcium and carbonate ions which nourish lateral growth as periodic secretion and deposition of the organic intertile membranes restrict their flux to the lateral growth surfaces. Arrows A designate organic interlayer imaged by SEM; arrow B designates lateral boundary of tile (adapted from Meyers et al. [15]).

Fig. 11. a) Demineralized shell revealing randomly oriented chitin fibrils from intertile layers; b) schematic representation of organic intertile layer composed of chitin fibrils. c) Schematic structure of chitin.

growth mechanism of aragonite tiles by retarding, periodically, the growth in the *c* axis direction.

- The results presented here strongly support the mechanism of periodic chitin layer deposition, retarding the growth of aragonite in the *c* direction and forming the organic intertile layers. Cavernous channels within the epithelium are identified and proposed to be sites for chitin synthesis.

Acknowledgements

This research is supported by the National Science Foundation Grant DMR 0510138 and UCSD Alliance for Graduate Education and the Professoriate Fellowship. We thank Ryan Anderson and Chung-Ting Wei for their assistance at Calit2 facility. Thanks go to Eddie Kisfaulady for maintenance of the open water facility and the feeding of abalone. Yen-Shan Lin provided aid in demineralization procedure. We thank Maribel Montero (CalIT2) for helping with AFM measurements. Assistance provided by Aruni Suwarnasarn with the scanning electron microscopy is greatly acknowledged.

References

- [1] M. Sarikaya, *Microsc. Res. Tech.* 27 (1994) 360.
- [2] A.V. Srinivasan, G.K. Haritos, F.L. Hedberg, *Appl. Mech. Rev.* 44 (1991) 463.
- [3] G. Mayer, *Science* 310 (2005) 1144.
- [4] C. Sanchez, H. Arribart, M.M. Giraud-Guille, *Nat. Mater.* 4 (2005) 277.
- [5] G. Mayer, M. Sarikaya, *Exper. Mech.* 42 (2002) 395.
- [6] M.E. Launey, E. Munch, D.H. Alsem, H.B. Barth, E. Saiz, A.P. Tomsia, R.O. Ritchie, *Acta Mater.* 57 (2009) 2919.
- [7] E. Munch, M.E. Launey, D.H. Alsem, E. Saiz, A.P. Tomsia, R.O. Ritchie, *Science* 322 (2008) 1516.
- [8] S. Deville, E. Saiz, R.K. Nalla, A.P. Tomsia, *Science* 311 (2006) 515.
- [9] S. Deville, E. Saiz, A.P. Tomsia, *Biomaterials* 27 (2006) 5480.
- [10] G. Bevelander, H. Nakahara, in: M. Omori, N. Watabe (Eds.), *The Mechanisms of Biomineralization in Animals and Plants*, Tokai University Press, Tokyo, 1980, p. 19.
- [11] K. Wada, *Biomineralization* 6 (1972) 84.
- [12] H. Nakahara, *Venus* 38 (1979) 205.
- [13] G. Bevelander, H. Nakahara, M. Kakei, *Venus Jpn. J. Malac.* 41 (1982) 33.
- [14] H. Nakahara, *Calcification of gastropod nacre*, in: P. Westbroek, E.W. De Jong (Eds.), *Biomineralization and Biological Metal Accumulation*, D. Reidel Publishing Company, Dordrecht, Holland, 1982, p. 225.
- [15] A. Lin, M.A. Meyers, *Mater. Sci. Eng. A* 390 (2005) 27.
- [16] M.A. Meyers, A.Y.M. Lin, P.Y. Chen, J. Muyco, *J. Mech. Beh. Bio. Mat.* 1 (2008) 76.
- [17] M.A. Meyers, C.T. Lim, A. Li, B.R. Hairul Nizam, E.P.S. Tan, Y. Seki, J. McKittrick, *Mat. Sci. Eng. C* 29 (2009) 2398.
- [18] H. Nakahara, in: S. Suga, H. Nakahara (Eds.), *Mechanisms and Phylogeny of Mineralization in Biological Systems*, Springer-Verlag, New York, 1991, p. 343.
- [19] H. Mutvei, in: M. Omori, N. Watabe (Eds.), *The Mechanisms of Biomineralization in Animals and Plants*, Tokai Univ. Press, 1980, p. 49.
- [20] M. Fritz, A.M. Belcher, M. Radmacher, D.A. Walters, P.K. Hansma, G.D. Stucky, D.E. Morse, *Nature* 371 (1994) 49.
- [21] M. Fritz, D.E. Morse, *Col. Int. Sci.* 3 (1998) 55.
- [22] A.M. Belcher, X.H. Wu, R.J. Christensen, P.K. Hansma, G.D. Stucky, D.E. Morse, *Nature* 381 (1996) 56.
- [23] A.M. Belcher, E.E. Gooch, in: E. Bauerlein (Ed.), *Biomineralization: From Biology to Biotechnology and Medical Application*, Wiley-Interscience, Germany, 2000, p. 221.
- [24] X.Y. Shen, A.M. Belcher, P.K. Hansma, G.D. Stucky, D.E. Morse, *J. Bio. Chem.* 272 (1997) 32472.
- [25] T.E. Schäffer, C. Ionescu-Zanetti, R. Proksch, M. Fritz, D.A. Walters, N. Almqvist, C.M. Zaremba, A.M., *Chem. Mater.* 8 (1996) 679.
- [26] A.M. Belcher, B.L. Smith, G.D. Stucky, D.E. Morse, P.K. Hansma, *Chem. Mater.* 9 (1997) 1731.
- [27] C.M. Zaremba, A.M. Belcher, M. Fritz, Y. Li, S. Mann, P.K. Hansma, D.E. Morse, J.S. Speck, G.D. Stucky, *Chem. Mater.* 8 (1996) 679.
- [28] M. Sarikaya, K.E. Gunnison, M. Yasrebi, J.A. Aksay, *Mater. Res. Soc.* 174 (1990) 109.
- [29] M. Sarikaya, J.A. Aksay, in: S. Case (Ed.), *Results and Problems in 'Cell Differentiation in Biopolymers'*, Springer, Amsterdam, 1992, p. 1.
- [30] M. Sarikaya, *J. Microscopy Res Techn.* 427 (1994) 360.
- [31] A.Y.M. Lin, P.Y. Chen, M.A. Meyers, *Acta Biomater.* 4 (2008) 131.
- [32] H.D. Espinosa, J.E. Rim, F. Barthelat, M. Buehler, *Prog. Mater. Sci.* 54 (2009) 1059.
- [33] A.G. Checa, J.H.E. Cartwright, M.-G. Willinger, *Proc. Natl Acad. Sci. USA* 106 (2009) 38.
- [34] J. Bezares, R.J. Asaro, M. Hawley, *J. Struct. Biol.* 163 (2008) 61.
- [35] J. Bezares, R.J. Asaro, M. Hawley, *J. Struct. Biol.* 170 (2010) 484.
- [36] A. Steinarsson, A.K. Imsland, *Aquaculture* 224 (2003) 353.
- [37] H.A. Lowenstam, S. Weiner, *On Biomineralization*, Oxford U Press, 1989.
- [38] K. Simkiss, K. Wilbur, *Biomineralization, Cell Biology and Mineral Deposition*, Academic Press, 1989.
- [39] A.M. Belcher, E.E. Gooch, *Protein components and inorganic structure in shell nacre, Biomineralization*, Wiley-Vch, New York, 2000, p. 221.
- [40] L. Addadi, D. Joester, F. Nudelman, S. Weiner, *Chem. Eur. J.* 12 (2006) 980.
- [41] M. Rousseau, E. Lopez, P. Stempflé, M. Brendlé, L. Franke, A. Guette, R. Naslain, X. Bourrat, *Biomaterials* 26 (2005) 6254.
- [42] M.A. Crenshaw, H. Ristedt, in: N. Omori, N. Watabe (Eds.), *The Mechanisms of Biomineralization in Animals and Plants*, Tokay U. Press, 1976.
- [43] S. Weiner, W. Traub, *FEBS Lett.* 111 (1980) 311.
- [44] S. Weiner, W. Traub, *Phyl. Trans. Roy. Soc. B.* 304 (1984) 421.